Electrostatic Analysis for Osmotic Flow through Rectangular Channels

Masako SUGIHARA-SEKI*, Takeshi AKINAGA*, Tomoaki ITANO*
and Teruo MATSUZAWA**

* *Department of Pure and Applied Physics, Faculty of Engineering Science, Kansai University, Suita, Osaka*
** *Japan Advanced Institute of Science and Technology, Nomi, Ishikawa*

An electrostatic model for osmotic flow through channels with surface charges is developed to understand the contribution of electrical charges to the transport of solution through narrow channels. The interaction energy between surface charges of the solute and the channel wall is used to express the osmotic reflection coefficient as a function of the surface charges, the ion concentration of the fluid, and the size ratio of the solute to the channel. Our model predicts that even for small Debye length compared to the channel size, the surface charges could significantly increase the osmotic flow, when the charges of the solute and the channel wall have the same sign.

1. INTRODUCTION

In biological systems, there are a variety of porous structures through which solutions consisting of solutes and suspending fluid are transported. Among them, it has been known for long time that many of the principal permeability properties of the capillary wall for water and water-soluble solutes can be well described in terms of flow through water-filled pores [1]. Since biological molecules are often electrically charged, significant contributions of electrical charges to the material transport have been reported for capillaries in various tissues [2,3]. For example, Adamson et al. [4] showed that for similar size solutes, ribonuclease and α–lactalbumin, the permeability of ribonuclease with positive charge was twice of that of α–lactalbumin with negative charge in frog mesenteric capillaries. Electrostatic effects are also pronounced in the material transport through artificial devices, such as electrophoresis and electroosmosis in a number of membrane separation and microdevice mixing processes [5].

In the present paper, we study theoretically the effect of electrical charges on the transport of solution through pores. Focusing on the osmotic flow of suspending fluid, driven by the difference in solute concentration across both ends of the pore, we develop an electrostatic model for the flow through the pore when the pore wall and the solutes have electrical surface charges and the suspending fluid is an electrolyte. We examine the dependence of the osmotic flow on the surface charges as well as the ion concentration of the electrolyte.

2. FORMULATION AND METHODS

We consider a membrane with long pores placed between two solutions differing in concentration. When the membrane is semipermeable, that is, only solvent can enter the pores of the membrane, a net volume flux of the solvent is expected, which is termed the osmotic flow. If the solutes are only partially excluded from the membrane, then the solvent flux J_v can be expressed in terms of the pressure difference Δp_∞ and the osmotic pressure $\Delta\Pi_\infty$ across the membrane, in such a way that

$$J_v = L_p(\Delta p_\infty - \sigma \Delta \Pi_\infty), \tag{1}$$

where the coefficient L_p is called the hydraulic conductivity and σ is the reflection coefficient (Kedem-Katchalsky equation) [2]. Note that $\sigma = 1$ for semipermeable membranes and σ tends to 0 as the solute size approaches 0. In the present study, we analyze how the reflection coefficient σ varies in the presence of electrical surface charges.

2.1 Expression for osmotic reflection coefficient σ

The pore is taken to be a uniform channel with rectangular cross-section of side lengths $2d_y$, $2d_z$ and length L ($>> d_y, d_z$), and its surface has uniformly distributed electrical charges with density q_c (figure 1). We consider the osmotic flow through the channel, when there are differences in pressure, $\Delta p_\infty = p_{0\infty} - p_{L\infty}$, and solute concentration, $\Delta c_\infty = c_{0\infty} - c_{L\infty}$, across both ends of the channel. The solutes are identical rigid spheres (radius a) with uniformly distributed surface charges (density q_s), and they are suspended in an electrolyte. The sizes of ions in the electrolyte are assumed to be small compared to both of solute size and channel size so that the electrolyte is regarded as a continuum, i.e. an incompressible Newtonian fluid. The viscosity of the fluid is represented by μ. The solution is assumed to be dilute enough that the interaction between the solutes can be neglected.

We take the x-axis along the centerline of the channel, and denote the fluid velocity as $\boldsymbol{u}=(u,v,w)$, the concentration of the solutes as $c = c(x,y,z)$, and the potential for the solute as $\phi(x,y,z)$. $\phi(x,y,z)$ is defined relative to the bulk phase where its value is zero. Thus, the Stokes equation is expressed as [6]

$$-\nabla p + \mu \nabla^2 \boldsymbol{u} - c \nabla \phi = 0. \tag{2}$$

Since the cross-section of the channel is uniform and the length L is much larger than the size of the cross-section, d_y or d_z, we can assume that $|u| >> |v|, |w|$ and $\phi = \phi(y,z)$. Under these assumptions (for details, see Anderson & Malone [6]), we obtain the simplified equation for the axial velocity from equation (2):

$$-\frac{\partial p}{\partial x} + \mu \left(\frac{\partial^2}{\partial y^2} + \frac{\partial^2}{\partial z^2} \right) u = 0. \tag{3}$$

For the velocity components in the cross-section of the channel, equation (2) leads to the approximate equations:

$$\frac{\partial p}{\partial y} + c \frac{\partial \phi}{\partial y} = 0, \quad \frac{\partial p}{\partial z} + c \frac{\partial \phi}{\partial z} = 0. \tag{4}$$

Note that equation (4) represents the mechanical equilibrium in the cross-section, indicating generation of pressure gradient in the y- and z-directions. If we further assume thermodynamic equilibrium, we have the Boltzmann distribution of the solutes such as

$$c(x,y,z) = c_0(x) \exp\left[-\frac{\phi(y,z) - \phi(0,0)}{RT} \right], \tag{5}$$

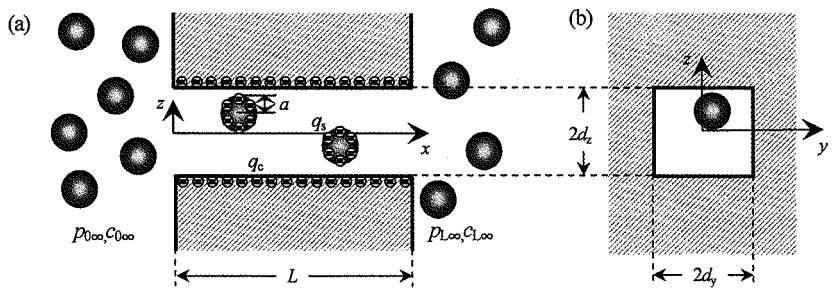

Fig. 1 (a) A sketch of the osmotic flow through channels with rectangular cross-section of side lengths $2d_y$, $2d_z$ and length L ($>> d_y, d_z$). Spherical solutes with radius a are suspended in an electrolyte. The surfaces of the channel wall and the solutes are electrically charged with density q_c and q_s, respectively. (b) Cross-sectional view.

where $c_0(x)$ represents the concentration on the x-axis, R is the gas constant and T is the absolute temperature. Substitution of equation (5) into equation (4) and subsequent integration yields

$$p(x,y,z) = p_0(x) - \Pi_0(x)\{1 - \exp[-(\phi(y,z) - \phi(0,0))/RT]\}, \tag{6}$$

where $\Pi_0(x) = RTc_0(x)$, representing the osmotic pressure on the channel centerline. This equation illustrates the coupling between solute concentration and pressure which generates the driving force for bulk flow. Then, from equation (3), we obtain

$$\mu\left(\frac{\partial^2}{\partial y^2} + \frac{\partial^2}{\partial z^2}\right)u = p_0' - \Pi_0' + \Pi_0' \exp\left[-\frac{\phi(y,z) - \phi(0,0)}{RT}\right], \tag{7}$$

where the prime represents d/dx. Since this equation is linear in u, its solution can be expressed in the form that

$$u(x,y,z) = [p_0' - \Pi_0'](-U_1) + \Pi_0' \exp[\phi(0,0)/RT](-U_2). \tag{8}$$

or

$$u(x,y,z) = -p_0' U_1 + \Pi_0' U^*, \quad U^*(y,z) = U_1 - \exp[\phi(0,0)/RT]U_2, \tag{9a,b}$$

where $U_1(y,z)$ and $U_2(y,z)$ are the solutions of the following equations:

$$\mu\left(\frac{\partial^2}{\partial y^2} + \frac{\partial^2}{\partial z^2}\right)U_1 = -1, \quad \mu\left(\frac{\partial^2}{\partial y^2} + \frac{\partial^2}{\partial z^2}\right)U_2 = -\exp\left[-\frac{\phi(y,z)}{RT}\right]. \tag{10a,b}$$

We apply the no-slip condition on the surface of the channel wall for U_1 and U_2. Apparently from equations (9a) and (10a), $U_1(y,z)$ represents the flow due to a constant pressure gradient along the channel axis, while $U^*(y,z)$ represents the osmotic flow driven by a gradient of the osmotic pressure Π_0'. We see from equation (10b) that $U_2(y,z)$ originates from the solute-wall interaction $\phi(y,z)$, which induces variation of the driving force in the channel cross-section. It should be noted for the osmotic flow that the first term of equation (9b), U_1, is the flow in the direction from dilute to concentrated side of the membrane, while the second term is in the opposite direction. Thus, the osmotic flow could occur in both directions across the membrane, depending on the solute-wall interaction $\phi(y,z)$.

By integrating equation (9) over the cross-section of the channel, S (= $4d_y d_z$), we have the flux of the solution through the channel, U, as

$$U = -p_0' Q_1 + \Pi_0'(Q_1 - \exp[\phi(0,0)/RT]Q_2), \tag{11}$$

where

$$Q_1 = \frac{1}{S}\int_S U_1 dS, \quad Q_2 = \frac{1}{S}\int_S U_2 dS. \tag{12a,b}$$

Note that U is the mean velocity averaged over the cross-section of the channel, and its value is constant independent of x, by continuity condition. Thus, equation (11) may be directly integrated along the x-axis from the channel entrance ($x = 0$) to the exit ($x = L$) to obtain

$$U = \frac{Q_1}{L}\{(p_0(0) - p_0(L)) - (\Pi_0(0) - \Pi_0(L))[1 - \exp(\frac{\phi(0,0)}{RT})\frac{Q_2}{Q_1})]\}. \tag{13}$$

By the use of the differences in the bulk values $\Delta p_\infty = p_{0\infty} - p_{L\infty}$ and $\Delta\Pi_\infty = \Pi_{0\infty} - \Pi_{L\infty} = RT(c_{0\infty} - c_{L\infty})$(see figure 1), equation (13) finally reduces to equation (1):

$$J_v = \alpha U = L_p(\Delta p_\infty - \sigma\Delta\Pi_\infty), \tag{14}$$

where

$$L_p = \alpha Q_1 / L, \quad \sigma = 1 - (Q_2/Q_1), \tag{15a,b}$$

and α is the pore volume fraction of the membrane [6].

If the channel has a circular cross-section, instead of rectangular one considered here, we see from equation (10a) that the velocity U_1 coincides with a Poiseuille flow driven by a unit pressure gradient. In this case, we have $Q_1 = r^2/8\mu$ for the pore radius r, in agreement with Anderson and Malone [6]. Correspondingly, for a fluid flow through rectangular channels when a unit pressure gradient is applied, an analytical solution for equation (10a) and the flow rate are given by [7]

$$U_1(y,z) = \frac{d_z^{\,2}}{\mu}\left(\frac{8}{\pi^2}\right)^2 \sum_{i=1,3,5,\cdots}\sum_{j=1,3,5,\cdots} \frac{(-1)^{(i+j)/2-1}}{ij\left((id_z/d_y)^2 + j^2\right)} \cos\left(\frac{i\pi y}{2}\right)\cos\left(\frac{j\pi z}{2}\right), \tag{16a}$$

$$Q_1 = \frac{2d_z^{\,2}}{\mu}\left(\frac{8}{\pi^2}\right)^3 \sum_{i=1,3,5,\cdots}\sum_{j=1,3,5,\cdots} \frac{1}{i^2 j^2\left((id_z/d_y)^2 + j^2\right)}. \tag{16b}$$

Here, we refer to the maximum velocity of U_1 as U_0, i.e. $U_0 = U_1(0,0)$, for later use.

On the other hand, equation (10b) does not have analytical solutions except some special cases. In general, we need to solve equation (10b) numerically, for given potentials ϕ. If the electrical charges are absent, the steric condition gives

$$\phi = \begin{cases} 0 & \text{for } |y| < d_y - a \text{ and } |z| < d_z - a \\ \infty & \text{for } |y| > d_y - a \text{ or } |z| > d_z - a \end{cases} \tag{17}$$

After substituting equation (17) into equation (10b), we solve the resultant equation and perform the integration of equation (12b). Then, we can get the value of σ from equation (15b), corresponding to the reflection coefficient when the electrical effects are absent. Apparently, σ is a function of the size ratios a/d_y and a/d_z. When there are surface charges on the channel wall and the solute, it depends also on the surface charges and the ion concentration in the electrolyte. In this case, we need at first to evaluate the potential energy ϕ for the solute in the presence of surface charges. The procedures to obtain ϕ are outlined in the following section.

2.2 Interaction energy

We consider dilute solution of spherical solutes suspended in an electrolyte. Neglecting the mutual interaction between the solutes, we treat a single solute whose center is placed at (y,z) in the cross-section of the channel (see figure 1(b)). In this section, we shall show how to evaluate the potential energy $\phi(y,z)$ from the electrostatic interaction energy between the solute surface charge (density q_s) and the channel surface charge (density q_c).

Inside the channel, the electrical potential Ψ is determined by the Poisson- Boltzmann equation [5,8,9]:

$$\nabla^2\Psi = -\frac{F}{\varepsilon}(z_+C_+ + z_-C_-), \tag{18}$$

where C_+, C_- represent the concentration of cation and anion, respectively, z_+, z_- are their valences, ε is the solvent dielectric permittivity, and F is the Faraday constant. If we consider the case of q_s, $q_c < 0$, i.e. both of surface charges of the solute and the channel wall are negative, then the condition of the electrical neutrality is expressed by

$$\int_V Fz_+C_+\,dV + \int_{\partial V_c} q_c\,dS = \int_V Fz_+C_{0+}\,dV, \tag{19}$$

$$\int_V Fz_-C_-\,dV = \int_V Fz_-C_{0-}\,dV, \tag{20}$$

where V is the volume of the electrolyte in the channel and ∂V_c is the surface of the channel. $C_{0\pm}$ represent the bulk concentrations of cation and anion, which satisfy the conditions of $z_+C_{0+} + z_-C_{0-} = 0$. Specifically, for the case of $z_+ + z_- = 0$, we denote $C_{0+} = C_{0-} = C_0$. Here, we assume the equilibrium of ions, so that the Boltzmann distribution is realized:

$$C_\pm = C^*_\pm \exp[-Fz_\pm\Psi/RT], \tag{21}$$

where $C^*_\pm$ are constants which are determined from equations (19) and (20). If we assume $z_+C^*_+ + z_-C^*_- = 0$ and $|z_\pm\Psi| << RT/F$, then equation (18) can be approximately expressed as [8,9]

$$\lambda_D{}^2 \nabla^2 \Psi = \Psi , \tag{22}$$

where

$$\lambda_D = [\varepsilon RT / F^2 (z_+{}^2 C^*{}_+ + z_-{}^2 C^*{}_-)]^{1/2} . \tag{23}$$

This approximation is termed the Debye-Hückel approximation, and λ_D is called the Debye length [5, 8, 9]. In particular, for a univalent-univalent electrolyte, the Debye length becomes

$$\lambda_D = [\varepsilon RT / 2F^2 C_0]^{1/2} , \tag{24}$$

and $\lambda_D \approx 1$ nm for a 0.1 M aqueous solution at $T = 310$ K. Note that the Debye length represents a characteristic decay distance of the electrical potential from charged surfaces, as apparent from equation (22).

In the present analysis, we do not adopt the Debye-Hückel approximation, since the electrical potential is not necessarily small, and the approximation does not satisfy the condition of the electrical neutrality. Alternatively, we substitute equation (21) into equation (18) under the conditions of equations (19) and (20), and the resultant equation is adopted as the governing equation for Ψ.

Outside of the channel in the membrane and inside of the solute, we assume no electrical charges, so that the electrical potentials Ψ' and Ψ'' in their regions satisfy the Laplace equation:

$$\nabla^2 \Psi' = 0, \quad \nabla^2 \Psi'' = 0. \tag{25}$$

Equations (18) and (25) should be solved simultaneously subject to the boundary conditions:

$$\varepsilon \partial_n \Psi - \varepsilon' \partial_n \Psi' = -q_c , \ \Psi = \Psi' \qquad \text{on the channel surface,} \tag{26a,b}$$

$$\varepsilon \partial_n \Psi - \varepsilon'' \partial_n \Psi'' = -q_s , \ \Psi = \Psi'' \qquad \text{on the solute surface,} \tag{27a,b}$$

and the additional requirement that Ψ' be finite infinitely far from the channel. Here, ∂_n represents the derivative normal to the surface into the electrolyte region, and ε', ε'' are the dielectric permittivity of the membrane and the solute, respectively. In aqueous systems, typically $\varepsilon' / \varepsilon \approx 0.05$. Then, for simplicity, we assume that both of ε' and ε'' are negligibly small compared to that of the electrolyte, ε. This assumption greatly facilitates subsequent computations, because we need not solve equation (25) to evaluate the interaction energy.

In terms of the electrical potential, the electrostatic energy in the field at a constant charge density q on the surface ∂V is described by [8,9]

$$E = \int_{\partial V} dA \int_0^q \Psi \, dq . \tag{28}$$

Thus, the interaction energy, or excess free energy, between the solute and the channel can be expressed by [8,9]

$$\phi = E_{cs} - E_c - E_s , \tag{29}$$

where the subscript CS designates the case of both solute and channel wall are electrically charged, the subscript C denotes the case of only charged channel is present, and the subscript S denotes the case of only charged solute is present. For various positions (y,z) of the solute in the cross-section of the channel, we have computed the electrical potential according to the procedures mentioned above, and estimated the electrostatic energy of the three cases E_{cs}, E_c, and E_s, to get the values of $\phi(y,z)$.

2.3 Numerical procedures

The value of σ is obtained as a function of a, d_y, d_z, q_c, q_s and $C_{0\pm}$. The procedure is summarized as the following three steps.

(a) Evaluation of Ψ from equations (18)-(21) and (26), (27), for given a, d_y, d_z, q_c, q_s, $C_{0\pm}$ and various positions of the solute center (y,z).

(b) Evaluation of ϕ from equations (28) and (29) as a function of (y,z).

(c) Evaluation of σ from equations (10), (12) and (15b).

In step (a), equation (18) together with equations (19) - (21) was solved subject to the boundary conditions

(26a) and (27a), by a finite-element spectral method. The computational domain was divided into a number of elements with curved hexahedral shapes, within which the electrical potential was approximated by interpolation functions composed of N-th degree Chebyshev polynomials of the local coordinates. Special attention was paid in making elements near the boundaries of the channel wall and the solute surface, especially in the case of small Debye lengths. To determine an appropriate number of N which yields sufficient numerical accuracy, we examined the variation of Ψ when computations were consecutively made by increasing N. For 28 elements, four digits of the Ψ values at several representative sites remained unchanged when N was increased from 4 to 6, whereas five digits remained unchanged for an increment of N from 6 to 8. Thus, we adopted $N = 8$ in the current study. Correspondingly, the numerical integrations in the finite-element scheme were performed by the Gauss-Legendre formulae of 16th degree along each local coordinate.

In step (b), we also adopted the Gauss-Legendre formulae of 16th degree in the numerical integration appeared in equation (28). In step (c), we solved equation (10) by employing the finite-element spectral scheme with $N = 8$, which is similar to step (a), besides it is two-dimensional. To assess the accuracy of the numerical computation, we compared the solution of equation (10a) obtained by the present method with the analytical solution (equation (16a)). The relative error of the maximum velocity at the channel center was on the order of 10^{-9}. Similarly, the relative difference of the flow rate from the analytical solution (equation (16b)) was about 10^{-8}.

The present approach is sufficiently complex that we limit our analysis to the cases of q_c, $q_s \leq 0$, $z_+ = -z_- = 1$ and $d_y = d_z = d$, i.e. channels of squared cross-section. For the case of q_c, $q_s \geq 0$, we can treat the problem in parallel, by modifying the condition of electrical neutrality, i.e. equations (19) and (20).

3. RESULTS AND DISCUSSION

A representative result of the present numerical computations is shown in figure 2, where the velocity profiles of the osmotic flow $U^*(y,z)$ normalized by U_0 are plotted along the y-axis, for $a = 6$ nm, $d = 10$ nm and the ion concentration $C_0 = 0.01$, 0.04 and 0.10 M. The corresponding Debye lengths are 3.0, 1.5 and 0.95 nm, respectively, for aqueous solutions at 310K. The solid curves represent the cases of $q_s = q_c = -1.02 \times 10^{-2}$ C/m^2, and the dashed curves for $q_s = -0.50 \times 10^{-2}$ C/m^2 and $q_c = -1.02 \times 10^{-2}$ C/m^2. For comparison, the velocity profile U^* in the absence of surface charges ($q_s = q_c = 0$) and that of U_1 are also plotted by a thin dotted curve and a thin solid curve, respectively. Without the surface charges, only steric condition (equation (17)) is present. In this case, a nearly flat velocity profile for $y/d < 1\text{-}a/d$ (= 0.4) is observed in figure 2. This may be understood by substituting equation (17) into equation (10b) and comparing the resulting equation with equation (10a), together with equation (9b).

Figure 2 shows that the curve representing the velocity profile of the osmotic flow is shifted from the nearly flat one in the absence of surface charges up to the U_1 curve, following a decrease in the ion concentration C_0, or an increase in the Debye length. This trend may be accounted for by a rise in electrostatic interaction ϕ between negative charges on the solute and channel surfaces which is induced by an increase in the Debye length, since the Debye length represents a characteristic distance within which the surface charge affects the electrical potential. In other words, as the Debye length is increased, the surface charges on the channel wall and the solute interact more strongly, and therefore enhance the osmotic flow. Apparently, the charge effect is more enhanced for larger surface charges, as is seen from a comparison between dashed curves for $q_s = -0.50 \times 10^{-2}$ C/m^2 and the corresponding solid curves for $q_s = -1.02 \times 10^{-2}$ C/m^2. Similar tendency is observed for various values of surface charges on the channel as well as on the solute.

Using the velocities U_1 and U_2 obtained, one can estimate the reflection coefficient σ as a function of a, d, q_c, q_s and C_0. The obtained values of σ are plotted in figure 3 as a function of the solute radius relative to the channel size, a/d, for $d = 10$ nm and the ion concentration $C_0 = 0.01$, 0.02, 0.04 and 0.10 M. The σ value in the absence of surface charges is also plotted by a thin dotted curve, for reference. We see that the thin dotted curve is lower than any other curves, indicating that the repulsive electrostatic interaction between solute and channel surface charges enlarges the reflection coefficient σ. A monotonous increase of σ with increasing solute radius is observed for each ion concentration, and its increase rate is larger for smaller ion concentrations, or larger Debye length. This implies an increase in osmotic flow with increasing solute size and/or decreasing C_0.

To illustrate more clearly the dependence on the Debye length λ_D, we have plotted the reflection coefficient σ as a function of d/λ_D for three values of the relative solute size, in figure 4. At large ratios of d/λ_D, each curve of σ approaches asymptotically the corresponding value of no-charged case, or purely steric exclusion. The asymptotes are shown by dotted lines in figure 4. As d/λ_D decreases, σ increases gradually up to 1, indicating an increase in osmotic flow with increasing the Debye length. As already seen in figure 2, a comparison between the solid curves and the corresponding dashed curves indicates that larger surface charges enhance the osmotic flow, when the surface charge on the solute and the channel wall have the same sign.

In the present approach, we have obtained the interaction energy between the surface charges (steps (a) and (b)), by following mostly the way applied to a circular cylindrical pore in Smith & Deen [8,9]. A substantial difference is that we have adopted equation (18) together with the condition of the electrical neutrality, while Smith & Deen [8,9] utilized its linearized equation (22). We have compared the two methods of analyses using linearized and original nonlinear equations for the circular cylindrical pore, and found significant discrepancies of the results particularly when the Debye length is large and/or the relative solute size is large [10,11]. For pores of rectangular cross-sections as in the present study, the principle is identical so that analogous tendency is anticipated.

We have estimated the reflection coefficient for the surface charges of the same sign. It is interesting to consider an attractive interaction between oppositely charged surfaces. For some adsorption potentials present for the circular cylindrical pore cases, Anderson & Malone [6] reported their results of σ, and showed that adsorption may have a rather large effect on the reflection coefficient. They predicted even negative values of σ,

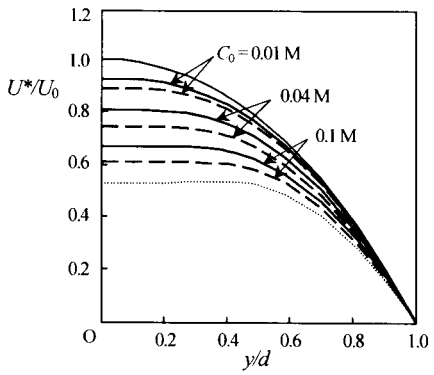

Fig. 2 The velocity profile of the osmotic flow U^* normalized by U_0 plotted along the y-axis, for various ion concentrations C_0 of an aqueous solution of a univalent-univalent electrolyte at 310 K with $a = 6$ nm and $d = 10$ nm. The velocity profile U^*/U_0 in the absence of surface charges ($q_s = q_c = 0$) and that of U_l/U_0 are also plotted by a thin dotted curve and a thin solid curve, respectively, for comparison.
In Figs. 2 - 4, the solid curves represent the cases of $q_s = q_c = -1.02 \times 10^{-2}$ C / m^2, and the dashed curves for $q_s = -0.50 \times 10^{-2}$ C / m^2, $q_c = -1.02 \times 10^{-2}$ C / m^2.

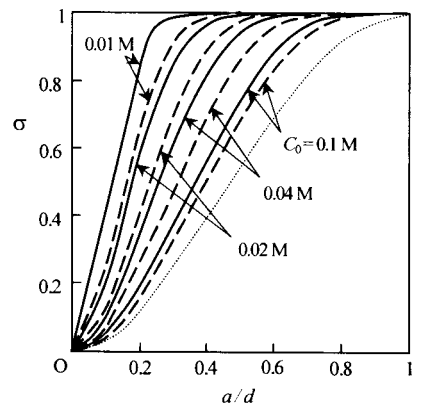

Fig. 3 Osmotic reflection coefficient σ for various ion concentrations C_0 of an aqueous solution of a univalent-univalent electrolyte at 310 K with $d =$ 10 nm. For reference, σ for steric condition alone is plotted by a thin dotted curve.

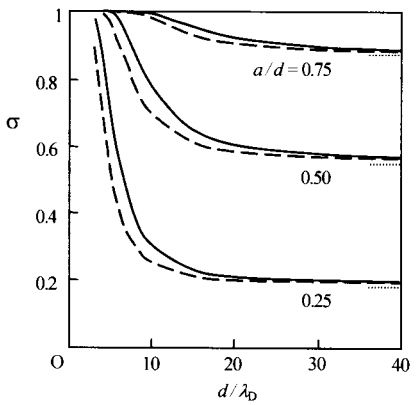

Fig. 4 Osmotic reflection coefficient σ against d/λ_D for the solute size $a = 2.5$, 5.0, 7.5 nm and $d = 10$ nm, in an aqueous solution of a univalent-univalent electrolyte at 310 K. The dotted lines indicate asymptotic values approached as d/λ_D tends to infinity.

implying a net flow in the direction from concentrated to dilute side of the membrane. Although they mentioned the presence of experiments showing such phenomena, it was concluded that their treatment should be restricted to a weak attraction between solute and pore wall. Similarly, our preliminary analysis for the surface charges of opposite sign in the present configuration has shown that the attractive interaction between the surface charges has an extremely large effect on σ even when the Debye length is relatively small. For instance, at C_0= 10 M (λ_D= 0.1 nm), we attain negative values of σ for a certain range of the relative solute size, with the other parameters being the same in figures 3 and 4. It is apparent that, as the attractive interaction becomes stronger, the solutes are more likely to approach the channel wall, so that the assumption of dilute solution employed here is invalidated near the channel wall. In this aspect, we need to clarify to what extent the present analysis can be applied to the case of surface charges of the opposite sign.

4. CONCLUDING REMARKS

We have developed an electrostatic model for osmotic flow through rectangular channels with surface charges. Our model predicts that if the solute and pore surfaces are electrically charged in the same sign, the interaction between them could significantly increase the osmotic flow through the pore, and this tendency is enhanced for larger Debye length and/or for larger surface charges.

Due to comparable sizes of a mean distance between adjacent water molecules of about 0.3 nm and a representative channel size of 20 nm considered in the current study, the best analysis would be performed on their molecular nature. One of most important differences from a continuum approach adopted here would be a possible presence of liquid slippage along the interface of liquid and solid phases. Another may be a formation of microclusters of water molecules. Despite recent significant developments of molecular-dynamics simulations and experiments, little is definitely known regarding these issues. Thus, the current study has been performed based on continuum mechanics under the conventional no-slip boundary condition on the solid surface. Future information about the motion of water molecules near solid phase will help us improving the present analysis.

Acknowledgement This research has been supported in part by a Grand-in-Aid for Scientific Research (B) 16360093 and 16360090.

REFERENCES

1) Michel, C.C. and Curry, F.E., Microvascular Permeability. Physiol. Rev. 79 (1999), pp. 703-761.
2) Curry, F.E., Mechanics and Thermodynamics of Transcapillary Exchange. In: Handbook of Physiology (Am. Physiol. Soc., 1984), vol. 4 part 1, pp. 309-374.
3) Truskey, G.A., Yuan, F. and Katz, D.F., Transport Phenomena in Biological Systems. (Pearson Education Inc., 2004).
4) Adamson, R.H., Huxley, V.H. and Curry, F.E., Single Capillary Permeability to Proteins Having Similar Size but Different Charge. Am. J. Physiol. 254 (1988), pp. H304-H312.
5) Probstein, R.F., Physicochemical Hydrodynamics. (John Wiley & Sons, Inc., 2003).
6) Anderson, J.L. and Malone, D.M., Mechanism of Osmotic Flow in Porous Membranes. Biophys J. 14 (1974), pp. 957-982.
7) Fletcher, C.A.J., Computational Techniques for Fluid Dynamics. (Springer-Verlag, 1988), p.139.
8) Smith, F.G. III and Deen, W.M., Electrostatic Double-Layer Interactions for Spherical Colloids in Cylindrical Pores. J. Colloid Interface Sci. 78 (1980), pp. 444-465.
9) Smith, F.G. III and Deen, W.M., Electrostatic Effects on the Partitioning of Spherical Colloids between Dilute Bulk Solution and Cylindrical Pores. J. Colloid Interface Sci. 91 (1983), pp. 571-590.
10) Akinaga, T., Sugihara-Seki, M. and Itano, T., Electrical Charges Affect Osmotic Flow through Pores. JPSJ (to be submitted).
11) Akinaga, T., Itano, T. and Sugihara-Seki, M., Transport of Charged Solutes through Charged Pores. Proceedings of the Annual Meeting of JSME 7 (2005), pp. 45-46 (in Japanese).